

Compressive and tensile strength of steel fibrous reinforced concrete under explosive loading

**A. S. Savinykh, G. V. Garkushin,
G. I. Kanel & S. V. Razorenov**

International Journal of Fracture

ISSN 0376-9429

Volume 215

Combined 1-2


Int J Fract (2019) 215:129-138

DOI 10.1007/s10704-018-00342-w



Your article is protected by copyright and all rights are held exclusively by Springer Nature B.V.. This e-offprint is for personal use only and shall not be self-archived in electronic repositories. If you wish to self-archive your article, please use the accepted manuscript version for posting on your own website. You may further deposit the accepted manuscript version in any repository, provided it is only made publicly available 12 months after official publication or later and provided acknowledgement is given to the original source of publication and a link is inserted to the published article on Springer's website. The link must be accompanied by the following text: "The final publication is available at link.springer.com".

Compressive and tensile strength of steel fibrous reinforced concrete under explosive loading

A. S. Savinykh · G. V. Garkushin  ·
G. I. Kanel · S. V. Razorenov

Received: 31 August 2018 / Accepted: 14 December 2018 / Published online: 1 January 2019
© Springer Nature B.V. 2019

Abstract In order to determine the compressive and tensile strength of concrete under conditions of explosive loading, and to develop a methodological framework in this regard, three types of concrete have been investigated: concrete with fine-grained granite in the form of crushed stone having a static compressive strength of 47 MPa, the same concrete with the addition of steel fibers and also the same concrete reinforced by steel bars. The samples were rods of 50 and 100 mm diameter and five to ten diameters in length. The compressive fracture occurs at a relatively small distance of propagation of the load pulse along the rod and is accompanied by fast decay. The measurements of parameters of the compression pulse at the end of the fracture zone allowed us to determine the values of the dynamic compressive strength of the concrete

while measurements of the free-surface velocity history at long distances were used for determining the dynamic tensile strength or spall strength values. The values of the dynamic compressive strength were found to be 2.5 times higher than the static strength. The steel fibers increased the dynamic compressive strength by about 10%. The obtained values of the dynamic tensile strength are 3–8 times higher than the values of the static tensile strength. The steel fibers increase the tensile strength by 20–50%. The reinforced sample has shown an increase of dynamic tensile strength by a factor of about 30.

Keywords Compressive strength · Tensile properties · Concrete · Fiber reinforcement · Explosive loading

1 Introduction

The problem of describing the dynamic strength of concrete is related to the necessity of the prediction of the resistance of the building structures to explosion, high-velocity impact or other intense pulsed actions. Concrete is a brittle material and its tensile strength is much lower than its compressive strength, and plastic deformation prior to fracture is negligible. The dynamic strength of brittle materials such as ceramics, minerals and glasses has been widely studied using the techniques employed in shock-wave experiments (Kanel et al. 2004). However, usually such experiments are carried out with the samples having characteristic sizes of several centimeters or even millimeters. A specific

A. S. Savinykh · G. V. Garkushin (✉) · S. V. Razorenov
Institute of Problems of Chemical Physics of the RAS,
Chernogolovka, Russia 142432
e-mail: garkushin@icp.ac.ru

A. S. Savinykh
e-mail: savas@icp.ac.ru

S. V. Razorenov
e-mail: razsv@icp.ac.ru

A. S. Savinykh · G. V. Garkushin · S. V. Razorenov
National Research Tomsk State University, Tomsk, Russia
634050

G. I. Kanel
Joint Institute for High Temperatures of the RAS, Moscow,
Russia 125412
e-mail: kanel@icp.ac.ru

requirement for the concretes is the necessity of the testing specimens having dimensions that are much greater than the sizes of structural heterogeneities that in a practical sense means tens of centimeters or meters. In our previous work (Savinykh et al. 2018), an attempt at the required enlarging of the scale of dynamic tests was made for a fine-grained concrete (rather for a mortar). In this paper, we present the results of further testing and development of the method (Savinykh et al. 2018). Three types of concrete were chosen as the materials to be tested: the concrete with fine-grained granite in the form of crushed stone (hereinafter, granite crushed stone) the same concrete with the addition of steel fibers, and the same concrete reinforced with steel bars. In addition, one more experiment was undertaken with concrete which has been the focus of an earlier study (Savinykh et al. 2018).

The fibers should noticeably increase the strength of concrete. Thus, it was found in Jiao et al. (2009) that with the addition of 3% of the volume fraction of steel fibers, the dynamic strength of concrete at strain rates between 40 and 100 s⁻¹ increased by approximately 30%. In Nili et al. (2016), it has been shown that 1% of the volume fraction of steel fibers with curved ends resulted in an increased resistance to the cracking under quasi-static and dynamic loadings. In Bazhenov (1970), the samples with the asbestos fibers were tested, and it was found that the Dynamic Increase Factor (DIF) defining the ratio of strength of concrete under dynamic loading to its static strength increased by 8–12% under tension and by 20–30% under shear stresses. On the other hand, in Coppola et al. (2011) the study of the strength properties of mortar with the addition of glass fibers and carbon nanotubes was conducted and it was found that the DIF for these mixtures was even lower than the DIF for the mortar having no fibers.

2 Materials and experiments

We investigated three kinds of fine-grained concrete, including the fiber-reinforced concrete and the concrete with reinforcing bars. All of the samples were prepared in the shape of rods of two different diameters, each having a length of 10 diameters. The components of incident mixtures were combined in the following proportions: for 1 kg of cement there was 1.4 kg of sand, 2.9 kg of granite in the form of crushed stone and 0.46 l of water. Portland cement (ExtraCEM 500, Holcim

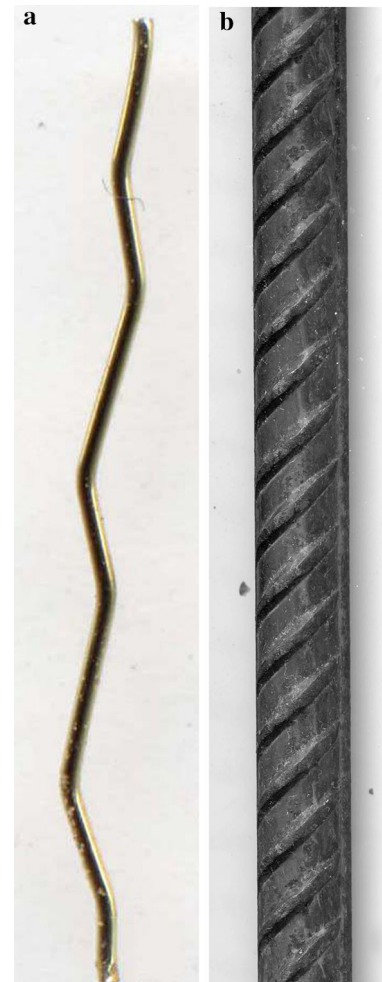


Fig. 1 a The steel wave fiber; b Steel rebar diameter: 8 mm

Group Services Ltd.) was used. The granite crushed stone had the particle size in the range from 2 to 5 mm. The weight of steel fibers for 1 kg of the mixture was 0.06 kg. The abovementioned proportion without the steel fibers corresponds to the brand cement M500 with a static compressive strength ~ 47 MPa. The steel wave fibers FSV-0.3/15 shown in Fig. 1a had a diameter of 0.3 mm and a length of 15 mm. The reinforcing steel bars shown in Fig. 1b had a diameter of 8 mm. Eight reinforcing bars were installed symmetrically at a distance of 20 mm from the outer surface, as shown in Fig 2.

The resulting mixture was poured into plastic pipes with diameters of 46 or 104 mm and lengths of 0.5 and 1 meter, respectively, after that all the workpieces of concrete mixtures were subjected to the vibration.

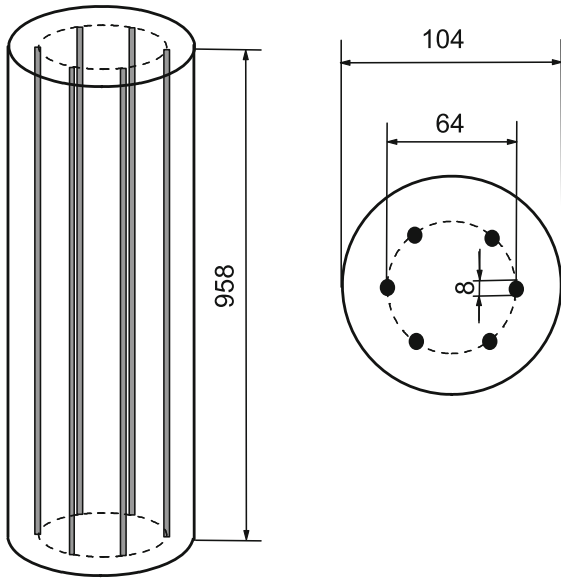


Fig. 2 The scheme of a reinforcing frame. Dimensions in figure are in mm

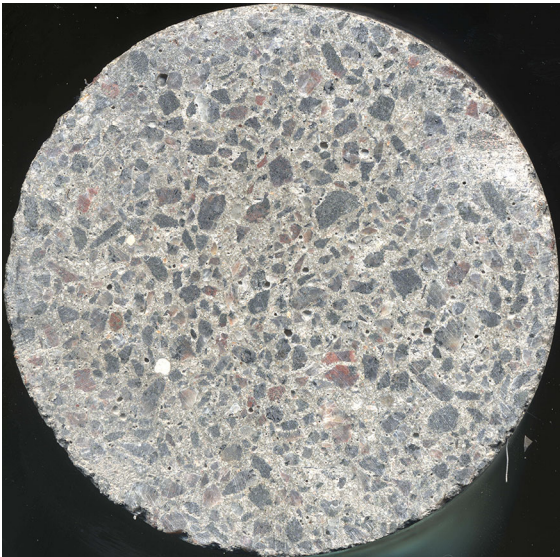


Fig. 3 The photo of the cross section of concrete rod of 104 mm in diameter

The samples were kept for more than 28 days in plastic pipes to prevent excessively rapid drying. Before the experiment, the pipe was removed and the rod ends were mechanically treated. The measured density of the concrete was 2.37 g/cm^3 for the basic concrete and 2.44 g/cm^3 for the fibrous concrete. The calculated density for reinforced concrete was 2.63 g/cm^3 . Figure 3 shows a photograph of the cross section of a concrete

rod which demonstrates the uniform distribution of the components and some moderate residual porosity of the material.

Figure 4 presents the scheme of the experiments. Detonation of the explosive lens with a diameter of 100 mm generated compressive pulses in the rod samples. The lens was placed in a steel ring in order to increase the load duration and uniformity. The initial load corresponds to uniaxial strain conditions. But, while the load pulse propagates along the rod the material is subjected to radial unloading and, as a result, at a sufficient distance from the input end the deformation mode of the rod in the compressive pulse approaches the uniaxial stress conditions. The measured output pressure of shock compression in the PMMA baseplate was 3.8 GPa; the shock pulse duration was longer than $10 \mu\text{s}$. A polarization detector of shock wave was placed between the baseplate and the sample in order to measure the pulse front propagation velocity. In the experiments, the velocity histories of the free rear ends of the rod samples were recorded by means of laser Doppler velocimetry in the form of the velocity interferometer system for any reflectors (VISAR) (Barker and Hollenbach 1972). In order to initiate and maintain the reflectivity of the sample end, aluminum foil of 400μ thickness was glued onto the output surface.

3 Compressive strength of concrete

Figures 5 and 6 present the free surface velocity histories for the concrete rods having two different diameters with and without steel fibers. Since no residual deformation was observed near the output ends of recovered rods, we assume that the compression wave becomes completely elastic at this distance. A reason for the long rise time of the compression wave is obviously associated with the wave scatter in the inhomogeneous material. The compression wave is followed by the unloading wave which causes a decrease in the velocity. Interaction of incident and reflected unloading waves leads to the generation of tensile stresses and spall fracture inside the rod. As a result, only a small initial part of unloading is recorded which is limited by the spall strength value. The stress relaxation at fracture creates a compression wave which appears on the free surface velocity history and causes the velocity increase.

Fig. 4 The scheme of experiments on the explosive loading of concrete rod samples

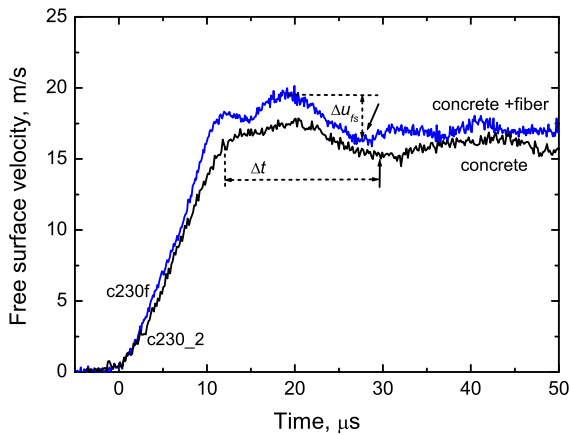
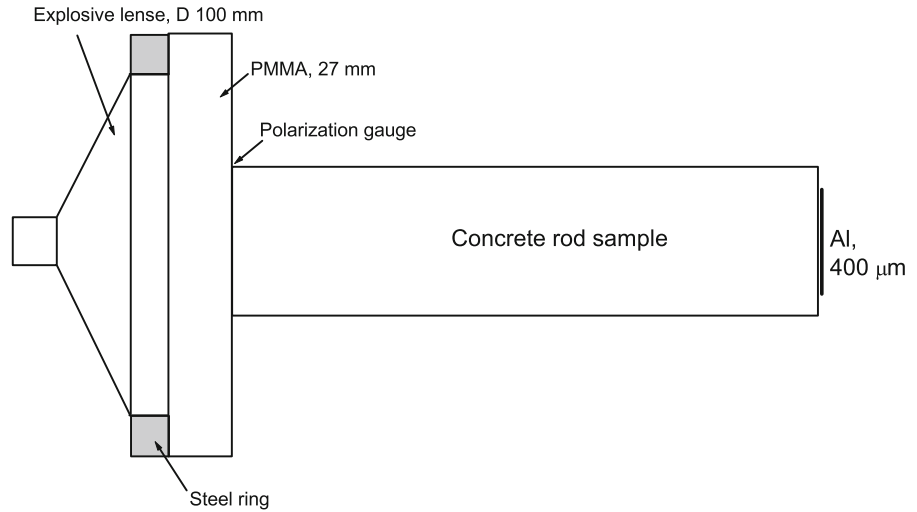


Fig. 5 The free surface velocity histories of concrete rods with the diameter of 46 mm and the length of ~ 230 mm. The arrows indicate the spall pulse front

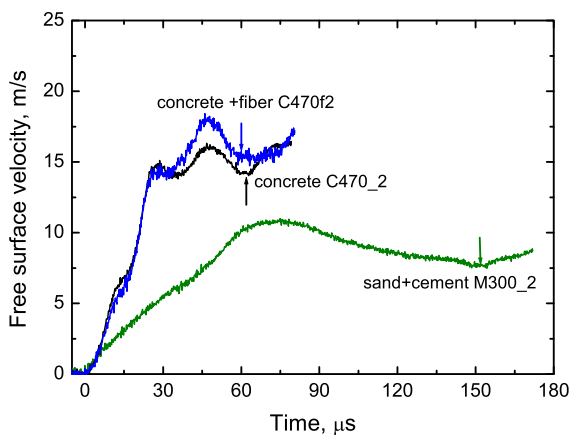


Fig. 6 The free surface velocity histories of concrete rods with the diameter of 104 mm and the length of ~ 470 mm. The arrows indicate the spall pulse front

The experimental data have a rather good reproducibility. In all of the experiments, the propagation velocity of the compression wave front was measured and was found to be equal to 3.99 ± 0.2 km/s for the concrete without fibers and 4.02 ± 0.2 km/s for the concrete with steel fibers. For comparison, Fig. 6 presents also the free surface velocity history of the M300 concrete rod of the same sizes. In accordance with previous work (Savinykh et al. 2018), the density of M300 is 2.1 g/cm^3 and the wave propagation speed is 3.6 ± 0.2 km/s. Although this concrete does not contain granite particles and it may be considered as less inhomogeneous, the waveform for this material demonstrates a much longer rise time. Probably, different rise times are the result of different viscosities due to the water content (Guo et al. 2017; Ozbolt et al. 2011). We used twice as much water per kilogram of final material for making M300 samples compared with M500. As a result, the porosity and perhaps residual water content were greater for M300.

Figures 7 and 8 show the photos of the sample rods that were recovered after the tests. The rear parts of the rods consist of several pieces separated by the abruptions or cracks, which are approximately perpendicular to the axis of the rod while the parts adjacent to the input end are formed by the inclined cracks which are typical for compressive fracture. The abruption is the result of the spallation. The recovered blocks have no residual traces of inelastic deformation.

The compressive fracture of the samples with a diameter of 46 mm takes place along a length of about 90–92 mm. Therefore, one can conclude that



Fig. 7 Samples of concrete rods with diameter of 46 mm after the test on dynamic compression. The material of upper rod is concrete with steel fibers (the shot number C230f), for the lower sample it is concrete (C230)

the compressive stress at this distance corresponds to the dynamic compressive strength of the concrete. For the rods of 104 mm diameter, compressive fracture occurred in the $171 \pm (10)$ mm long section in the case of pure concrete and in the $139 \pm (10)$ mm long section in the case of concrete with steel fibers. We can suppose that a longer fracture length means a larger compressive stress withstood by the material, which means that the steel fibers in the composition of concrete increase the compressive strength.

The following experiments have been performed with the rods of length being equal to the length of the fracture zone, that is 171 mm and 139 mm for the concrete and the concrete with a fibers, respectively, and diameters of 104 mm and 91 mm for the rods of smaller diameter. The measurements of the free surface velocity histories under the same loading conditions were carried out. The results are presented in Figs. 9 and 10. The influence of steel fibers on the recorded waveforms is not significant, nevertheless, it is seen that fibrous concrete sustains higher stress in spite of the longer distance for decay of the incident load pulse. The peak values of the velocity for the rods of two different diam-

eters do not differ much from each other, and this may be considered as confirmation of the correctness of this method of determining the fracture stresses.

Thus, the compressive stress defined by the measurements of free surface velocity histories for two kinds of concrete rods with different diameters should correspond to the dynamic compressive strength of these kinds of concrete. For calculations of the stresses, the values of the dynamic impedances ρc (here ρ is the density, c is the sound speed) are needed. In accounting for the small values of particle velocity and stresses, calculations may be performed using an acoustic approach while assuming that the density and sound speed are constant.

Since the compression wave broadens with propagation, the velocity of its middle part was taken for estimation of the dynamic impedance. For the wave profiles shown in Fig. 10, velocities were 3.55 ± 0.2 km/s for the concrete without fibers and 3.58 ± 0.2 km/s for the concrete with steel fibers. Because of the lack of information on the dynamic compressibility of the concrete, we assume in the usual manner that its dynamic impedance under the compression and sub-

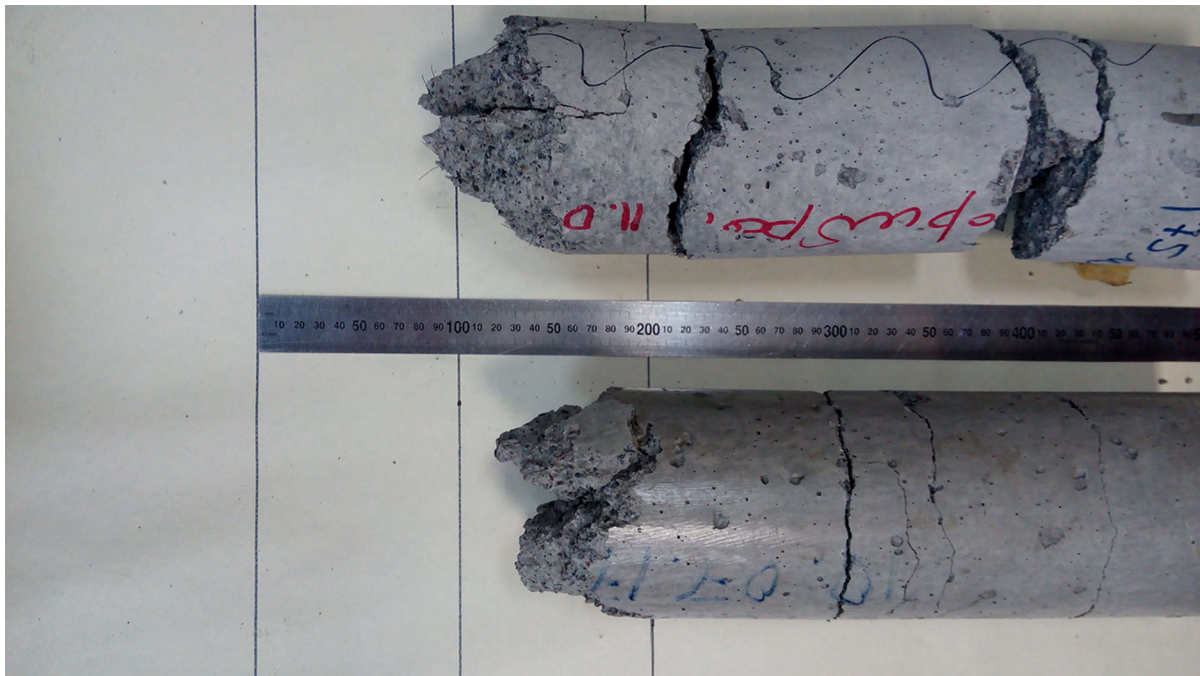


Fig. 8 Samples of concrete rods with diameter of 104 mm after test on dynamic compression. The upper sample is the concrete with steel fibers (C470f), for the lower sample it is concrete (C470)

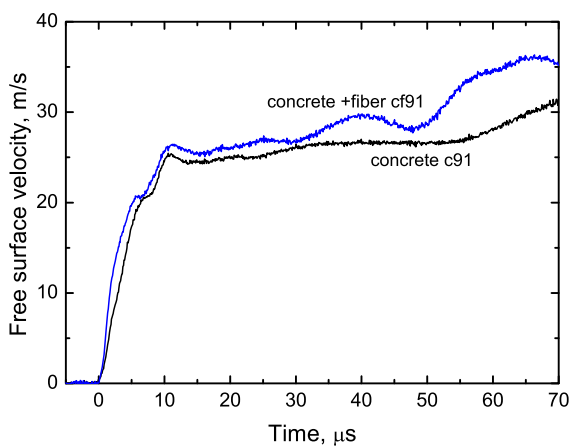


Fig. 9 The free surface velocity histories of the rods of concrete with and without steel fibers having a length of 91 mm and a diameter of 46 mm

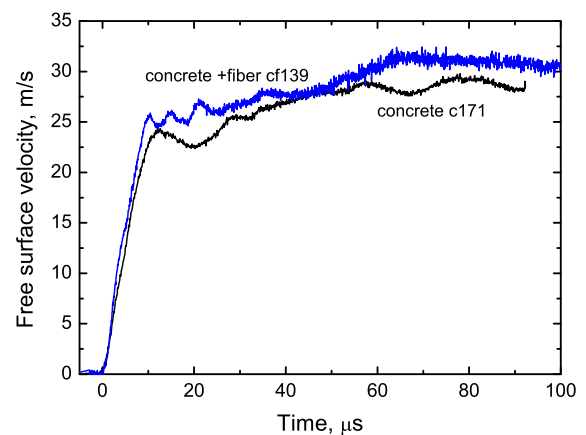


Fig. 10 The free surface velocity histories of the concrete rods of 104 mm in diameter with and without steel fibers having a length of 171 mm and 139 mm, respectively

sequent unloading remains unchanged. Under these assumptions, the compressive stress at the end of the fracture zone is defined as $\sigma = \rho c u_{fs}/2$, where u_{fs} is the peak free surface velocity in the compression wave. We used the peak value of the surface velocities because at this distance the materials sustain the whole compression pulse without fracture.

The stresses calculated in this way are summarized in Table 1. It can be seen that regardless of the diameter, the addition of steel fibers slightly increases the compressive strength. Since the compositions of the studied concretes correspond to the brand of concrete M500, it was assumed that the samples were characterized by the quasistatic compressive strength of the M500 which

Table 1 Dynamic compressive strength of the investigated concrete

Experiment	D (mm)	L (mm)	u_{max} (m/s)	σ_x (MPa)	DIF	$\dot{\epsilon}$ (s^{-1})
C171, concrete	104	171	29 ± 2	124 ± 8	2.63	344
Cf139, concrete + fiber	104	139	31 ± 2	132 ± 8	2.80	402
C91, concrete	46	91	31 ± 2	132 ± 8	2.80	471
Cf91, concrete + fiber	46	91	36 ± 2	153 ± 8	3.25	510

D rod diameter; L length of the rod

is equal to 47 MPa that is less than half of the measured dynamic strength. Mentioned in the Table 1 strain rates in the compression wave were calculated using the free surface velocity histories as $\dot{\epsilon} = \dot{u}_{fs}/2c$, where \dot{u}_{fs} is the velocity gradient in the compression wave. Also, the calculated Dynamic Increase Factor (DIF) of the investigated concrete under the duration of the loading of the order of 50–100 μs is presented in Table 1. The obtained values of DIF in the range of 2.5 to 3 for the concrete and for the concrete with steel fiber of two diameters at the strain rate of 350–500 s^{-1} agree with the available experimental data (Guo et al. 2017) on dynamic properties of concrete, including fine-grained concrete.

4 Dynamic tensile strength of the concrete

The interaction of incident and reflected unloading waves near the rod rear end results in the generation of tensile stresses and spall fracture inside the sample rod that appears in Fig. 11 as the approximate plane rupture cracks perpendicular to the rod axis. The measured lengths of the spalled pieces close to the end of the rod are presented in Table 2. These values are close to those that were evaluated from the free surface velocity histories using the relation (Kanel et al. 2004): $h = \Delta t/(1/c + 1/c_l)$, where Δt is the time interval between the spall pulse front and upper part of the compression wave as is shown in Fig. 5, c_l is the recorded propagation velocity of the compression wave. The lengths of the spall pieces calculated in this way are also presented in Table 2. Good agreement of the calculated and directly measured lengths of spall pieces of rods for the three types of concrete confirms the correctness of use of the wave dynamics.

By means of measuring the velocity pullback values Δu_{fs} on the free surface velocity histories shown in Figs. 5 and 6, it is possible to calculate the value of

the tensile stresses realized just before the spall fracture (the spall strength) using the relation (Kanel et al. 2004) $\sigma^* = \rho c \Delta u_{fs}/2$. The values of spall strength σ^* calculated in this way are also presented in Table 2. The propagation velocity of the mid-point of the compression wave for brand M300 is 2.1 ± 0.2 km/s (Savinykh et al. 2018). It is seen that the fibrous concrete possesses a spall strength that is much higher than the concrete without additives. The value of spall strength of the sand-cement mixture of brand M300, as expected, is the lowest. From the reference data it can be found that the quasistatic tensile strength of the cement brand M500 is 2.8 MPa, and the strength of the cement brand M300 is 2.1 MPa. In estimations of the DIF for tensile strength, it was assumed that the strength of the cement brand M500 and the concrete with steel fiber were equal under tension at the static loading. The results are presented in Table 2. It is seen that DIF is in the range from 3 to 8 when the strain rate under tension is from 15 to 70 s^{-1} , which agrees with the available experimental data (Bragov et al. 2015) on dynamic properties of concrete under high rates of tension.

Figure 12 presents the photo of the reinforced concrete rod with a diameter of 104 mm, a length of 958 mm that was recovered after the test. The axial part inside the reinforcing ring with a diameter of about 56 mm remained non-fractured; the compressive fracture has formed a conical surface at its end at a distance of 90 mm from the apex of the cone and at a distance of 130 mm from the base of the cone with a diameter of 56 mm. Under the action of explosive loading, the steel rebars were bent in the radial direction away from the axis of the rod. The right-hand side of Fig. 12 shows the symmetry of the deformation of the reinforcing frame relative to the rod axis. The destruction of the external concrete ring stopped at a distance of 310–350 mm. The whole recovered part does not visually contain any evidence of tensile fracture.

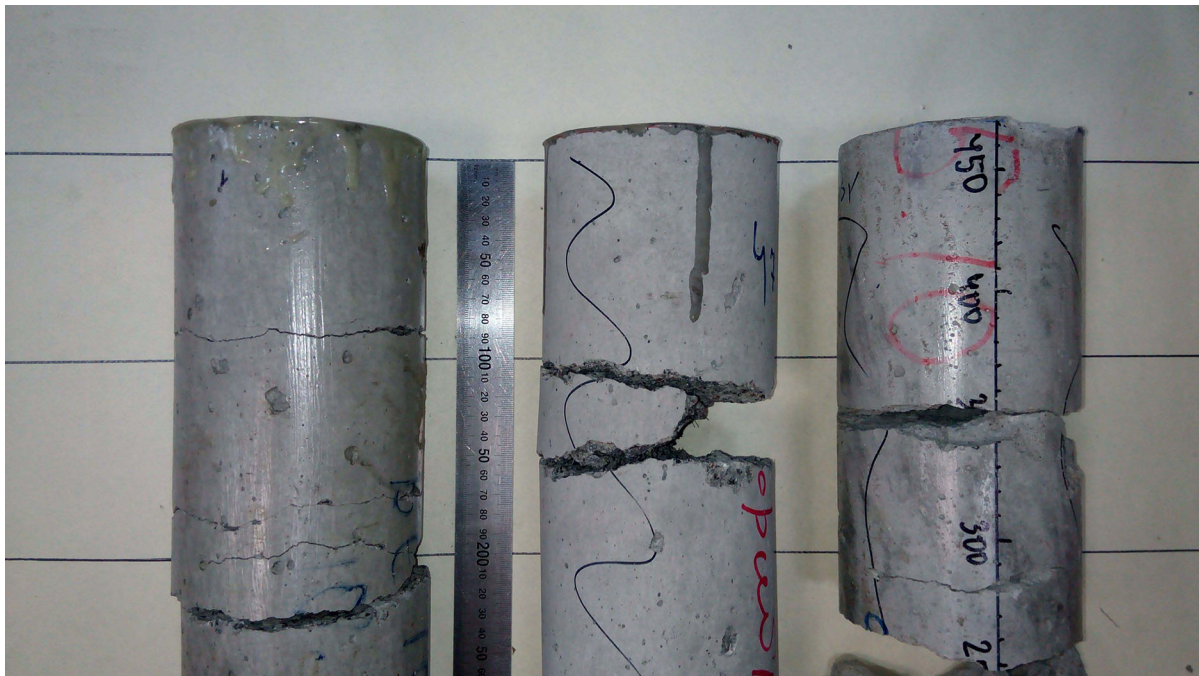


Fig. 11 The rear parts of the concrete rods with a diameter of 104 mm recovered after the tests. From left to right: concrete (C470), concrete with steel fiber (C470f), sand-cement mixture of brand M300 (M300_2)

Table 2 Dynamic tensile strength of the tested concrete

Experiment	D (mm)	L (mm)	Δu_{fs} (m/s)	σ^* (MPa)	h_{calc} (mm)	h_{real} (mm)	DIF	$\dot{\epsilon}$ (s^{-1})
C470, concrete	104	471	2.4	10.1	82	80–90	3.6	30
C470_2, concrete	104	475	1.9	7.9	71	78–90	2.8	31
C470f, concrete + fiber	104	475	5.5	24.2	108	100–110	8.6	28
C470f2, concrete + fiber	104	468	2.8	12.1	61	55–63	4.3	42
M300_2	104	471	3.1	6.83	116	110–120	3.3	15
C_ar, reinfor.concrete	104	958	16.2	> 81.5	–	no	29.1	15
C230_2, concrete	46	232	2.5	10.5	35	52–57	3.8	48
C230f, concrete + fiber	46	230	3.5	15.2	30	55–60	7.2	70

h_{calc} is an calculated thickness of spall plate, h_{real} the measured thickness of the spall plate

Figure 13 presents the free surface history recorded in the experiment with the reinforced rod. The steel reinforcing bars complicated the loading history as a result of which the recorded velocity went into the negative domain. The velocity of the wave front c_l that was registered using a polarizing gauge was 4.39 km/s. The estimation of the minimum possible value of spall strength was conducted using the recorded velocity pullback. The latter has been estimated as 16.2 m/s, also accounting for the part in the negative domain.

The estimations of spall strength for the reinforced rod are shown in Table 2. The calculated tensile strength of the reinforced sample was 7.5 times higher than that of the unreinforced concrete and 3–5 times higher than that of the concrete with steel fiber. The calculated DIF for the reinforced concrete was 29, which appears to be an overestimated value due to the large deviation from the one-dimensional motion of matter in the rod.

Fig. 12 Photographs of the reinforced concrete rod with a diameter of 104 mm, a length of 958 mm recovered after loading. Left—side view, right—top view

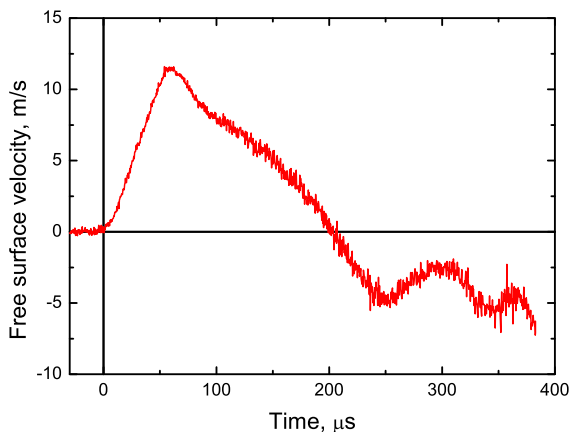


Fig. 13 The free surface velocity profile of the reinforced concrete with a diameter of 104 mm, a length of 958 mm (c_ar)

Conclusion

The performed experiments, as described in the present paper, with three types of concrete confirmed the workability and efficiency of the suggested method for evaluating the dynamic strength properties of concrete. The arrangement of tests with rods allows the use of rel-

atively large-scale samples. The obtained data are in reasonable agreement with each other and also with the data in the body of literature and show a significant increase of the resistance to fracture in comparison with the low-rate of response of the concrete.

Acknowledgements This work was performed with the support of the State Corporation “Rosatom” in the framework of the State contract 1 N.4 h.241.9B.17.1013 of February 20, 2017. The authors are grateful to A. V. Kulikov for the assistance in preparing and conducting experiments.

Funding This study was funded by the State Corporation “Rosatom” in the framework of the State contract 1 N.4 h.241.9B.17.1013 of February 20, 2017. Author Kanel G.I. has received research grants from the State Corporation “Rosatom”.

Compliance with ethical standards

Conflict of interest The authors declare that they have no conflict of interest. Corresponding author Garkushin Gennady confirms, on behalf of all authors, that the information provided is accurate.

References

- Barker LM, Hollenbach RE (1972) Laser interferometer for measuring high velocities of any reflecting surface. *J Appl Phys* 43:4669–4675. <https://doi.org/10.1063/1.1660986>
- Bazhenov YM (1970) Concrete under dynamic loading. Stroizdat, Moscow (in Russian language)
- Bragov AM, Igumnov LA, Lomunov AK (2015) High-rate deformation of fine-grained concrete and fiber reinforced concrete. Publishing House of Nizhny Novgorod University, Nizhny Novgorod
- Coppola L, Cadoni E, Forni D, Buoso A (2011) Mechanical characterization of cement composites reinforced with fiberglass, carbon nanotubes or glass reinforced plastic (GRP) at high strain rates. *Appl Mech Mater* 82:190–195. <https://doi.org/10.4028/www.scientific.net/AMM.82.190>
- Guo YB, Gao GF, Ling L, Shim VPW (2017) Response of high-strength concrete to dynamic compressive loading. *Internat J Impact Eng* 108:114–135. <https://doi.org/10.1016/j.ijimpeng.2017.04.015>
- Jiao C, Sun W, Huan S, Jiang G (2009) Behavior of steel fiber-reinforced high-strength concrete at medium strain rate. *Front Archit Civ Eng China* 3(2):131–136. <https://doi.org/10.1007/s11709-009-0027-0>
- Kanel GI, Razorenov SV, Fortov VE (2004) Shock-wave phenomena and the properties of condensed matter. Springer, New York. <https://doi.org/10.1007/978-1-4757-4282-4>
- Nili M, Ghorbankhani AH, AlaviNia A, Zolfaghari M (2016) Assessing the impact strength of steel fibre-reinforced concrete under quasi-static and high velocity dynamic impacts. *Constr Build Mater* 107:264–271. <https://doi.org/10.1016/j.conbuildmat.2015.12.161>
- Ožbolt J, Sharma A, Reinhardt HW (2011) Dynamic fracture of concrete compact tension specimen. *Int J Solids Struct* 48:1534–1543. <https://doi.org/10.1016/j.ijsolstr.2013.08.030>
- Savinykh AS, Garkushin GV, Kanel GI, Razorenov SV (2018) Method of measurement of the dynamic strength of concrete under explosive loading. *Int J Fract* 209(1–2):109–115. <https://doi.org/10.1007/s10704-017-0244-9>

Publisher's Note Springer Nature remains neutral with regard to jurisdictional claims in published maps and institutional affiliations.